AIAA SciTech Forum
5-9 January 2015, Kissimmee, Florida
56th AIAA/ASCE/AHS/ASC Structures, Structural Dynamics, and Materials Conference

10.2514/6.2015-0967

Modeling cure induced damage in fiber reinforced composites

Royan J. D'Mello, Marianna Maiarù and Anthony M. Waas*
Composite Structures Laboratory, Department of Aerospace Engineering,
University of Michigan, Ann Arbor, MI 48105, U.S.A
Folusho Oyerokun
GE Aviation, 1 Neumann Way, Cincinnati, OH 45215, USA
Li Zheng
GE Global Research, 1 Research Circle, Niskayuna, NY 12309, USA
Pavana Prabhakar
Department of Mechanical Engineering, University of Texas, El Paso, TX 79968, U.S.A

A novel computational model is introduced to analyze the effect of the curing process on the subsequent mechanical response of fiber reinforced composite structures. Evaluations are made at the microscale where representative volume elements (RVEs) are analyzed with periodic boundary conditions (PBCs) using the finite element (FE) method. The commercial software ABAQUS is used as a solver, supplemented by user written subroutines. The transition from a continuum to damage and failure is effected by using the Crack Band model which preserves mesh objectivity. Results are presented for a hexagonal packed RVE whose matrix portion is first subjected to curing and subsequently to mechanical loading. The effect of the fiber packing randomness on the microstructure is analyzed. It is noted that throughout the analysis, the possibility of failure is accommodated, i.e. failure can take place during the cure cycle and prior to application of mechanical loads under appropriate external conditions.

I. Introduction

Fiber-reinforced polymer composites (FRPCs) are high-strength and lightweight advanced materials widely used in aerospace engineering. An accurate understanding of the material state during cure is required for better characterization of the subsequent structural properties. The behavior of the matrix during curing can be altered by the presence of fibers and by details of the curing cycle. The system undergoes shrinkage due to chemical processes, and thus, builds self-equilibrating internal stresses. Depending on the constituent chemistry and thermal cycle that are used during curing, and the fracture and strength properties of a curing matrix, a fiber reinforced composite can and may undergo damage and cracking during the cure cycle. Moreover during this process, shrinkage in the matrix can affect the final shape of the structure. Song & Waas[1] showed that the use of "virgin" matrix properties in numerical predictions can lead to erroneous results for FRPCs. Thus, it is necessary to have accurate knowledge of the influence of cure cycle on the subsequent mechanical response of the laminate. In the present investigation, the damage at the microstructural level induced by curing is studied by first considering a hexagonally packed representative unit volume (RVE) having only a total of two fibers (one full center fiber and quarter fibers at four corners) and then a randomly packed configuration that has multiple fibers. Randomness is considered to quantify the variability in strength of the cured product.

The curing process can be divided into two parts: The first part consists of the chemical reaction, heat

*Author for correspondence: Felix Pawlowski Collegiate Professor of Aerospace Engineering, 1320 Beal Avenue, Ann Arbor, MI 48109; AIAA Fellow; email: dcw@umich.edu

generation and conduction. The second is the generation of self equilibrating stress and development of the structural integrity by evolution of the matrix stiffness. In the present paper, the curing of a thermoset polymer matrix is proposed. The stress generation is modeled as introduced earlier by Mei,[2] Mei et al.[3] and Heinrich et al.[4]

The degree of cure (ϕ) of the matrix is defined as $\phi = H(t)/H_r$, where $H(t)$ is the heat generated at time t, and H_r is the total heat of reaction. Then, the rate of cure can be defined as,

$$\frac{d\phi}{dt} = f(T, \phi) \tag{1}$$

where $f(T, \phi) \geq 0$ is a function. The evolution of temperature (T) and degree of cure (ϕ) for the matrix material system is determined through a coupled system that considers the heat equation and an empirical curing law or can be supplied from the output of a simulation that takes into account a cure kinetics model. A popular form of this empirical function has been provided by Kamal[5]

$$f(T, \phi) = \left[A_1 \exp\left(\frac{\Delta E_1}{TR}\right) + A_2 \exp\left(\frac{\Delta E_2}{TR}\right) \phi^m\right] (1 - \phi)^n \tag{2}$$

where T is temperature, R is the gas constant, ΔE_1 and ΔE_2 are activation energies. The constants A_1, A_2, m and n have to be determined by fitting the above equation to the experimental data. During curing, the material heats up due to exothermic chemical reaction and to the conduction from the heating source at the boundary. This process can be modeled using the governing equation[4]

$$\rho c \frac{\partial T}{\partial t} = \frac{\partial}{\partial x_i}\left(\kappa(T, \phi)\frac{\partial T}{\partial x_i}\right) + \rho H_r \frac{\partial \phi}{\partial t} \tag{3}$$

where ρ is the mass density, c_p is the specific heat and κ is the thermal conductivity.

The evolution of self-equilibrating stresses during curing is incorporated in the analysis by using a model proposed by Heinrich et al.[4]

$$\begin{aligned}\sigma_{ij}(t) = \int_0^t \frac{d\phi}{dt}\delta_{ij}[K(s)(\epsilon_{kk}(t) - \epsilon_{kk}(s) + 3\epsilon_c(s) - 3\alpha\Delta T(t, s)) \\ +2\mu(s)(\epsilon_{ij}(t) - \epsilon_{ij}(s) - \frac{\delta_{ij}}{3}\{\epsilon_{kk}(t) - \epsilon_{kk}(s) + 3\epsilon_c(s)\})]ds \\ +(1 - \phi(t))K(0)\delta_{ij}(\epsilon_{kk}(t) - 2\alpha(0)\Delta T(t))\end{aligned} \tag{4}$$

where K, μ, α and ϵ are the per-network bulk modulus, shear modulus, coefficient of thermal expansion and cure shrinkage respectively. Also, $K(0)$ and $\alpha(0)$ corresponds to the bulk modulus and coefficient of thermal expansion of the liquid resin. As shown by Heinrich et al.,[4] the per-network properties can be obtained from experimentally measured values of the plane wave modulus (M_{exp}), and shear modulus (μ_{exp}) for the curing matrix.

II. Hexagonally packed fiber RVEs

A 3D hexagonally packed RVE with volume fraction $V_f = 0.70$ is chosen for study, and subjected first to cure and next to mechanical loading. The latter leads to a determination of the transverse tensile strength, S_{22}^{+}. The analysis is done using commercially available finite element software ABAQUS/Standard. The RVE shown in figure 1 has width $w = 6.83$ μm, height $h = 11.8$ μm and thickness $t = 0.30$ μm. Carbon fibers are 6 μm in diameter. Both the fiber and the matrix are modeled as isotropic solids.

For sake of simplicity, this problem can be divided in three steps described as shown in figure 1. In Step I, a thermochemical analysis is performed using the cure parameters described in Hubert et. al.[6] Applying the curing cycle at the boundary, the degree of cure and the cure rate in the matrix are provided. Since the RVE dimensions are on the micron scale, it can be assumed that there is little to no variation in the temperature field across the RVE. Thus, temperature was prescribed on the entire volume at every time instance. The temperature profile applied for this case study and the degree of cure (ϕ) are shown in figure 2. Notice that the resin is partially cured at the end of the process, the maximum degree of cure is 0.83.

In Step II, the mechanical problem is solved and the stress evolution is computed. A crack band model is used to simulate cracking during the curing matrix, if it exists. During curing, the matrix gradually solidifies (stiffness increases) and simultaneously contracts (cure shrinkage) due to network formation. Residual

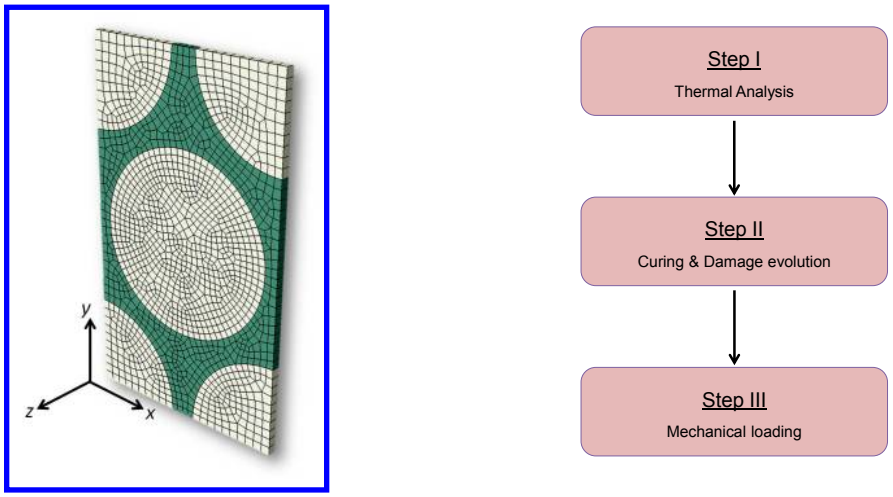

Figure 1. Hexagonally packed fiber-matrix RVE (left). Steps used in the present analysis (right).

stresses develop in the matrix owing to cure shrinkage and thermal strains. Depending on the magnitude of tensile stresses developed, the degree of cure (ϕ) and the rate of cure ($\frac{d\phi}{dt}$), the material may crack locally during curing. The critical tensile stress for cracking typically increases with the degree of cure. If certain matrix regions crack, it would result in a matrix material with reduced stiffness, which ultimately controls the tensile strength of the RVE. If a volume of material cracks, it is assumed that no further curing can take place in this cracked region. That is, it is assumed that cracking during the cure process leads to no further curing. At the end of Step II, the curing process is completed.

In Step III, the cured RVE (containing cracks or not, as the case maybe) is subjected to transverse tension loading along the x-direction (equivalently 2-direction in the material frame). The objective is to compute the RVE strength (S_{22}^{+}). Based on the temperature and cure parameters, computation of the stress evolution during cure (Step II) and strength calculation based on mechanical loading (Step III) is performed in a unified step in ABAQUS/Standard. In this work, it is assumed that cracking in the curing matrix can occur only for $\phi > 0.7$ and only under tensile stresses. A crack band model based on the one proposed by Bažant & Oh[7] is used to model failure in the matrix. Two representative critical stress values to failure (σ_{cr}) of 50 MPa and 70 MPa are chosen. Each of these values is assumed to be independent of ϕ. However it is expected that the strength would vary with ϕ. The critical Mode I energy release rate (G_{IC}) is chosen to be 0.6 N/mm. Stiffness evolution as a function of cure was taken from an epoxy system (Epon 862) described in Heinrich et al.[4] During curing and mechanical loading, the RVE is subjected to periodic boundary conditions, representing an infinite medium. During the cure cycle (Step II), the dimensions along the x-direction are constrained to remain fixed. However, the RVE boundaries can contract or expand in the other two directions.

The evolution of stress σ_x as a function of time during Step II is shown in figure 3. The stress reported here is the nominal stress measured on the positive x-face of the RVE. Positive value of σ_x indicates tensile stress. Compressive stresses first develop in the RVE during the first 8,500 seconds of the cure cycle. These are thermal stresses due to heating. Here, the effect of curing is negligible because the value of ϕ is close to 0. After $t = 8,500$ s, when ϕ rapidly increases, the stress σ_x become tensile. This behavior is due to cure shrinkage. Thereafter, a plateau is seen starting from $t = 11,500$ s up to $t = 15,700$ s. Here, there is no stress build up because curing is complete and no additional heating or cooling takes place between these time instances. Note that even though the value of ϕ is similar for all the regions in the matrix, the internal stresses are non-uniform because of non-uniform matrix geometry, which constraints various portion of the matrix by varying amounts. This stress non-uniformity is shown in figure 4 for two time instances, the first during heating cycle (at $t = 8,250$ s) and the other when cure is in progress (at $t = 10,000$ s) for the $\sigma_{cr} =$ 50 MPa simulation. Cracking starts when the maximum principal stresses in some elements approach σ_{cr}. The onset and spread of microcracks in the matrix is shown in red in figure 5. By the end of the curing cycle, we have a partially damaged RVE owing to formation of micro-cracks during the curing process. The extent

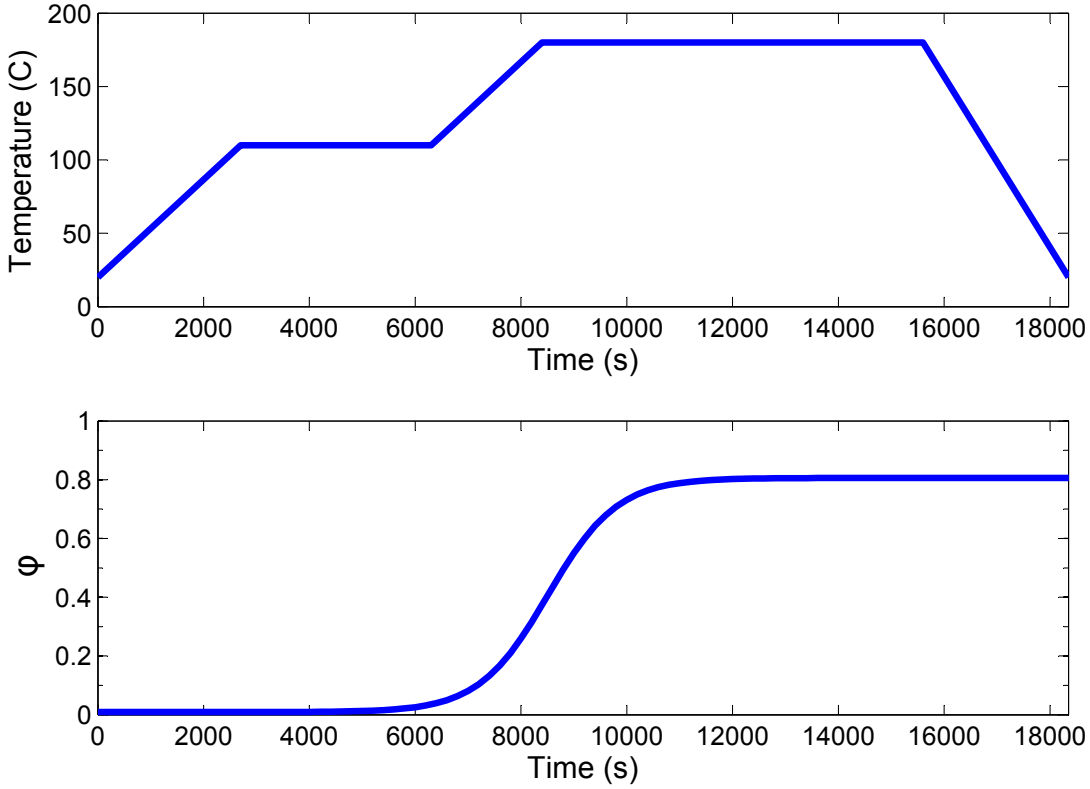

Figure 2. Temperature profile (top) and degree of cure (bottom) as functions of time.

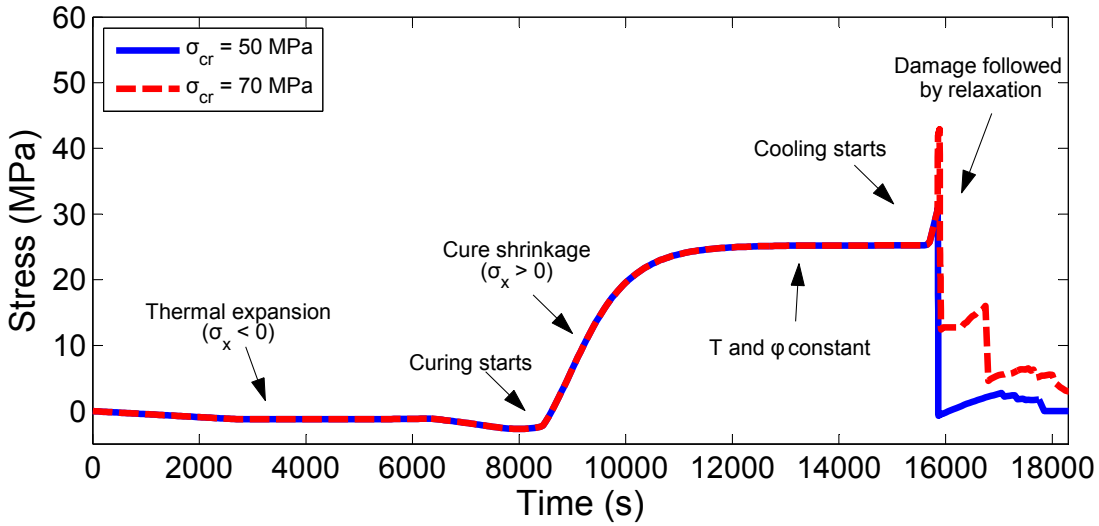

Figure 3. Stress evolution during cure shown using nominal stress σ_x as a function of time.

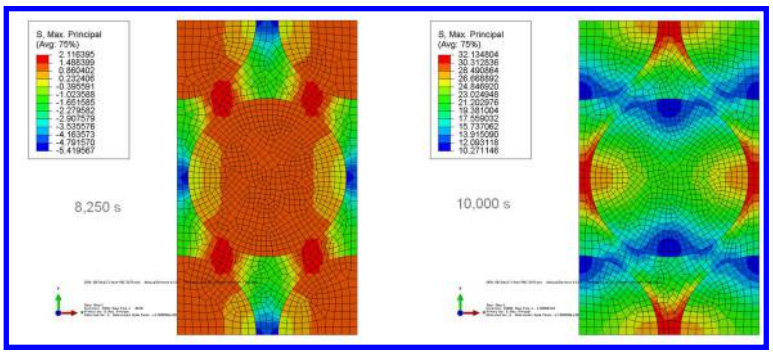

Figure 4. Map of maximum principal stresses in the RVE at two time instances: $t = 8,250$ s, during the initial heating step (left) and, (b) $t = 10,000$ s, when curing has started (right).

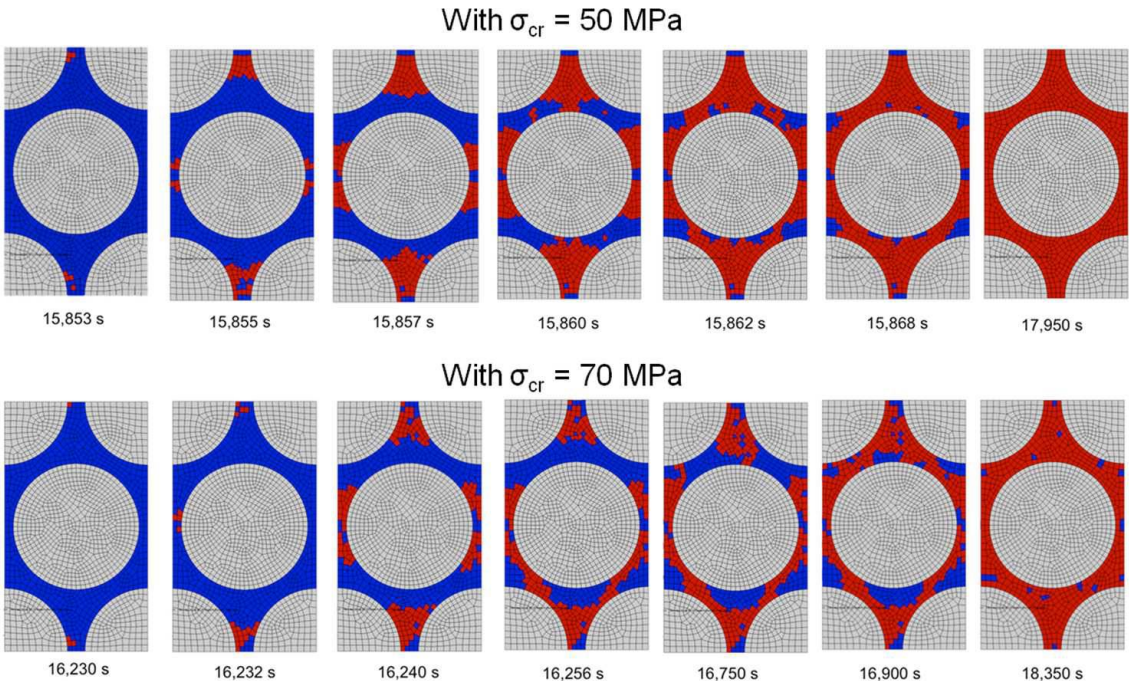

Figure 5. Spread of damage during curing (Step II). Red regions indicate the presence of damage.

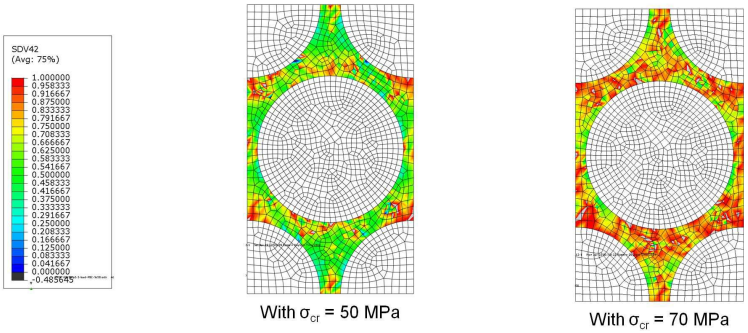

Figure 6. Extent of damage (D) in the matrix at the end of the curing cycle (Step II) for $\sigma_{cr} = 50$ MPa and $\sigma_{cr} = 70$ MPa. Here, $D = 1$ corresponds to no damage while $D = 0$ corresponds to complete damage (two-piece failure).

of damage in the RVE can be quantified as a stiffness knockdown factor D. That is, $D = 1$ would mean that the there is no damage locally in the matrix due to formation of microcracks and hence no reduction in stiffness. Thus, $D = 0$ would indicate that locally, the matrix has lost all its stiffness and has completely failed (two-piece failure). The map of D at the end of the cure cycle with $\sigma_{cr} = 50$ MPa and $\sigma_{cr} = 70$ MPa is shown in figure 6. It is seen that RVE with $\sigma_{cr} = 50$ MPa has more damage compared to that with $\sigma_{cr} = 70$ MPa, which is expected.

The stress-strain responses for the hexagonal packed RVE with $\sigma_{cr} = 50$ MPa and $\sigma_{cr} = 70$ MPa, respectively, are shown in figure 7. Also shown are the crack paths in red for the two RVEs. Before the peak is attained, some nonlinearity is present in the response. This nonlinearity can be attributed to previously damaged regions in the matrix (in Step II) that have reduced stiffness. Past the peak, there is a significant drop in the stress, which is similar to the failure of a brittle solid. The peak strengths in both these simulations are close to their critical strength value of σ_{cr}.

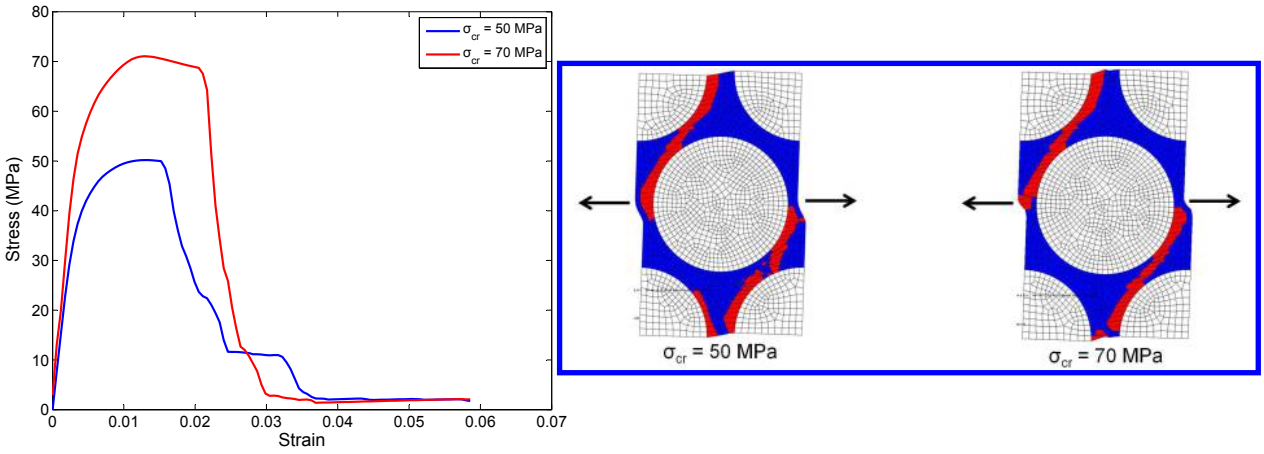

Figure 7. Stress-strain response of the RVE in the x-direction corresponding to $\sigma_{cr} = 50$ MPa and $\sigma_{cr} = 70$ MPa. Also shown are the crack paths in red for the two RVEs.

III. Random Fiber RVEs

The effect of fiber packing in the microstructure has also been studied by analyzing different renditions of a square RVE with volume fraction $V_f = 0.55$ that have 20 randomly packed fibers. The cure cycle applied on these RVEs and stiffness evolution in the matrix as a function of cure are similar to those used in the 2-fiber RVE described in the previous section. The critical fracture stress σ_{cr} is selected to be 30 MPa. The RVEs have been modeled as square cells in the $x - y$ plane (which is equivalent to the 2-3 plane in the material frame) where the dimension of the side is $l = 32$ μm and the thickness $t = 0.3$ μm. Carbon fibers are 6 μm in diameter and are randomly distributed within the RVEs. The cross-section of the 10 different renditions used in this analysis is shown in figure 8. As in the previous case, both the fiber and the matrix are modeled as isotropic using 3D solid elements.

Two outlier RVEs are also studied. Inspection of the actual microstructure of fiber-reinforced laminates shown the presence of several matrix rich pockets. Thus, Model 11 has been built having a matrix rich region at the center of the RVE and is shown in figure 8. The fibers in the rest of the region are randomly packed but maintaining an overall volume fraction $V_f = 0.55$. Additionally, slight material inhomogeneity has been introduced by including four weaker elements (with $\sigma_{cr} = 25$ MPa) at the edge of the matrix rich region. Model 12 is that of an idealized hexagonally packed RVE where 16 fibers have been included. The geometry of this RVE is different from the other 11 renditions since it is hexagonally packed. This rectangular cell has width $w = 38.8$ μm, height $h = 26.7$ μm and thickness $t = 0.3$ μm.

The aim of this analysis is threefold: (a) to determine how the transverse tensile strength (S_{22}^{+}) of the idealized hexagonally packed RVE differs from more realistic configuration where fibers are randomly placed within the RVE; (b) to quantify the variation in the strength value within RVEs that have randomly packed fibers; (c) to study how the presence of an extended region of matrix affects strength.

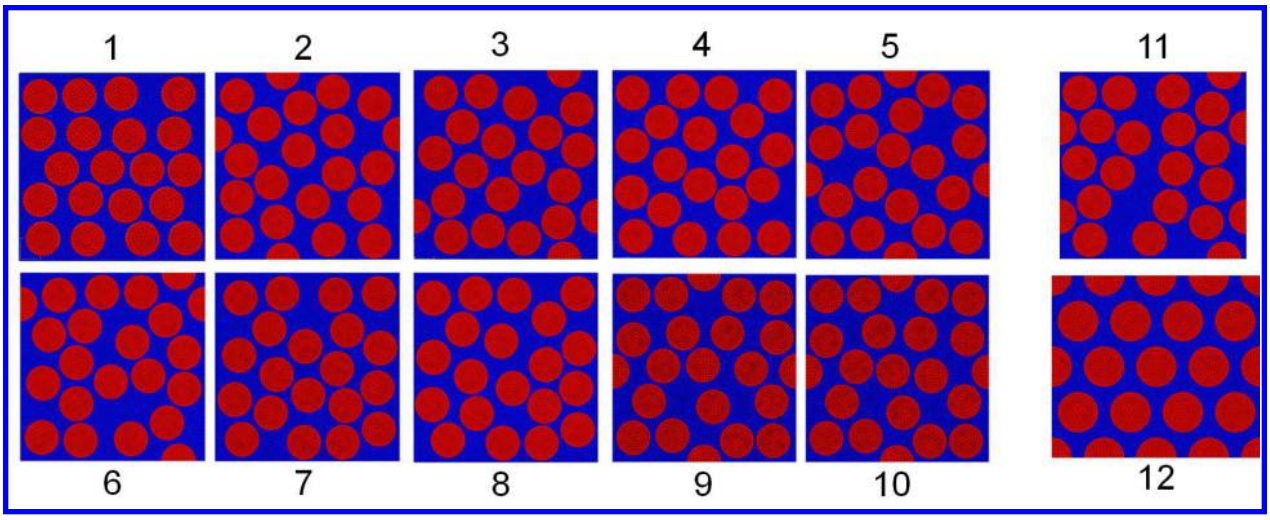

Figure 8. Renditions of randomly packed RVEs (1-11). The random packed RVE (11) has a matrix rich region in the middle. The hexagonally packed RVE (12) is also shown.

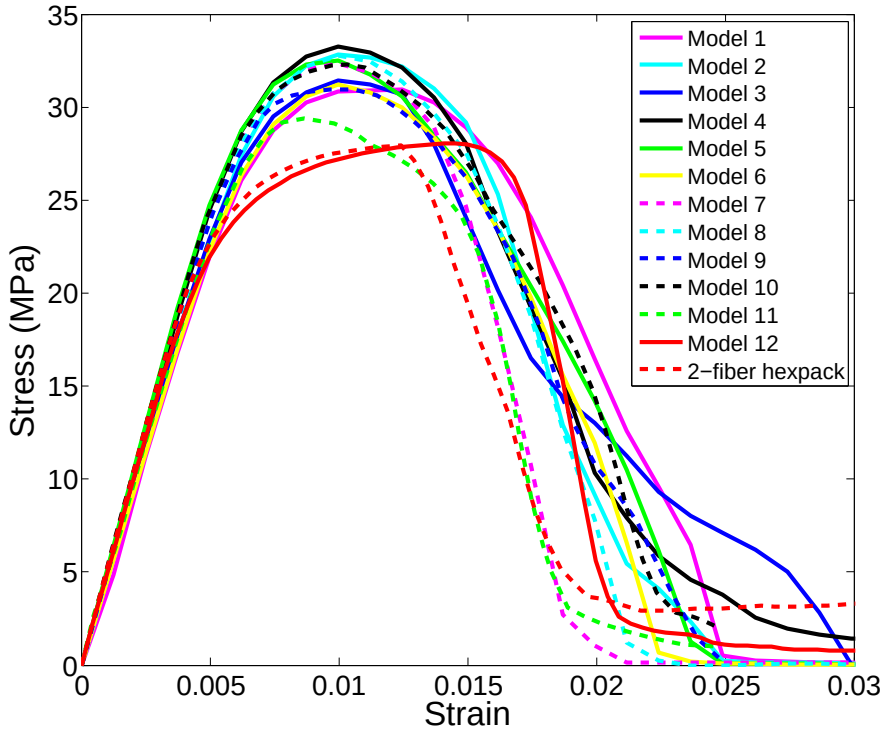

Figure 9. Stress-strain response for the proposed RVEs.

After these 12 RVEs have been subjected to the cure cycle and loaded in tension along the transverse direction, the resulting stress-strain response is shown in figure 9. Here, the 16-fiber hexagonally packed cell has also been compared with the 2-fiber hexagonally packed RVE. The S_{22}^{+} strength values for the 12 models considered in this study are shown in figure 10. The hexagonal packed cells appear to be the lower limit compared to the different renditions, except the matrix enriched one (Model 11). Thus, results provided by the hexagonally packed cell are conservative compared to the randomly packed renditions. As will be shown, this behavior is due to the fact that the crack path in a randomly packed RVE tends to be more tortuous than in a hexagonally packed RVE. Also shown in figure 10 is the strength distribution. The mean strength is 31.5 MPa with standard deviation 1.5 MPa. The strength distribution is negatively skewed. It is interesting to note that the strength value of the 16-fiber hexagonally packed RVE (Model 12) is similar to that of a 2-fiber hexagonally packed RVE having the same volume fraction $V_f = 0.55$.

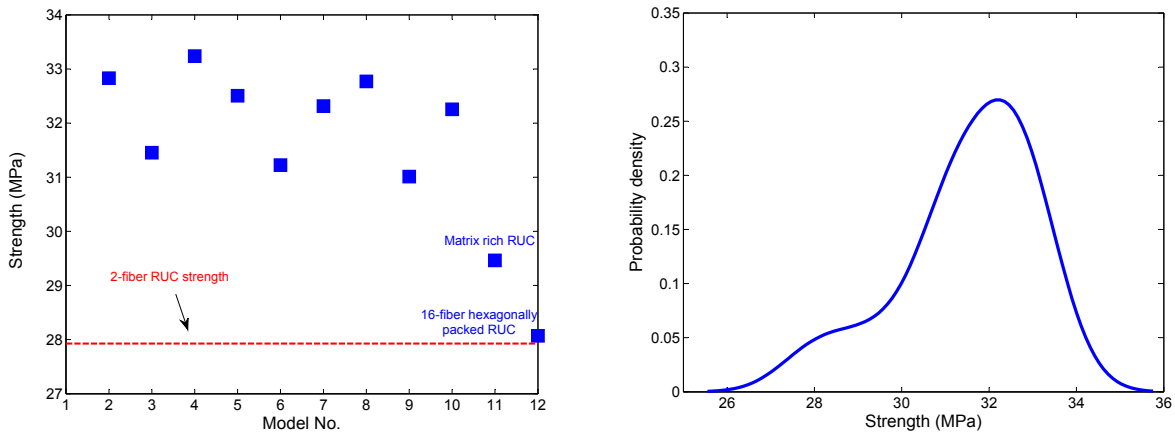

Figure 10. S_{22}^{+} strength values for the 12 models (left). Strength distribution (right).

The crack initiation site is different for each RVE. To better explain the crack propagation, the maximum principal strain map for three models is studied. Figure 11, 12 and 13 show the evolution of the maximum principal strain during Step III for Model 1, Model 11 (with the matrix rich region) and Model 12 (hexagonally packed). The crack initiation site, which is influenced by fiber packing can influence the subsequent crack path in the RVE. Figure 14 shows images of the final crack path in each of the RVEs. It is interesting to note that the crack initiation site for the Model 11 was unaffected by the location of the weaker elements (in the matrix rich region) which were added to introduce material non homogeneity in the RVE. The failure initiation point here is caused instead by the stress concentration due to the tightly packed fibers away from the matrix rich region and not at the few weaker elements introduced in the matrix rich region.

Once a crack has initiated, fibers can be seen as obstacles that the crack has to avoid in order to propagate. The more tortuous the crack path, the higher is the strength value. It is expected that the crack path in a randomly packed RVE is in general, more tortuous compared to a uniform configuration such as the hexagonal packing (Model 12). This explains the fact that the hexagonal packed RVE (Model 12) had the lowest strength when compared to all the other randomly packed fiber RVEs (Models 1-11).

IV. Conclusion and Future Work

The effect of the cure cycle and its influence on subsequent mechanical response in FRPC RVE models has been studied using the network model proposed by Heinrich et al.[4] in conjunction with the crack band model. Hexagonal packed RVE results have been compared with those of randomly packed RVEs. It is seen that the transverse strength (S_{22}^{+}) of the virtually cured RVE depends on the fiber packing. Estimates for the variability of strength has been provided for the RVEs studied in this paper. Using the approach described here, several cure cycles can be considered and eventually tailored to reduce damage in the microstructure during the cure process, leading to a desired mechanical strength of the cured product. Since fiber packing is seen to influence strength of the cured RVE, it would be interesting to study the correlation of strength

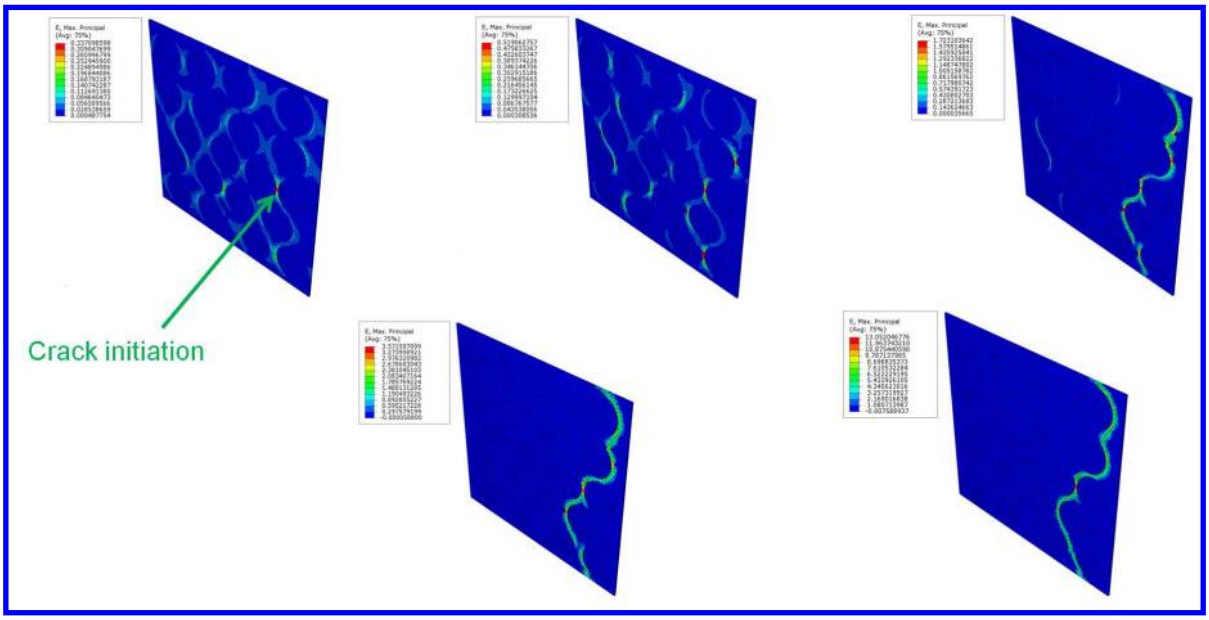

Figure 11. Contour plots of maximum principal strain in Step III along with initial crack initiation site for random RVE - Model 1).

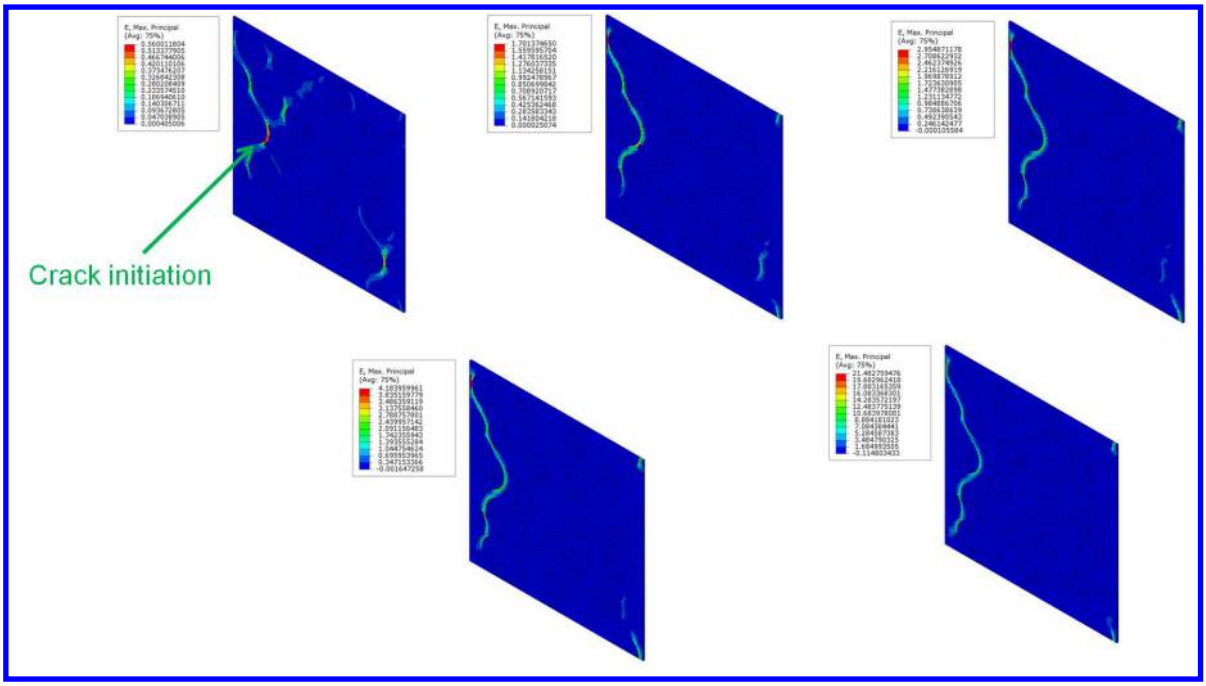

Figure 12. Contour plots of maximum principal strain in Step III along with initial crack initiation site for random RVE - Model 11 (having matrix rich region).

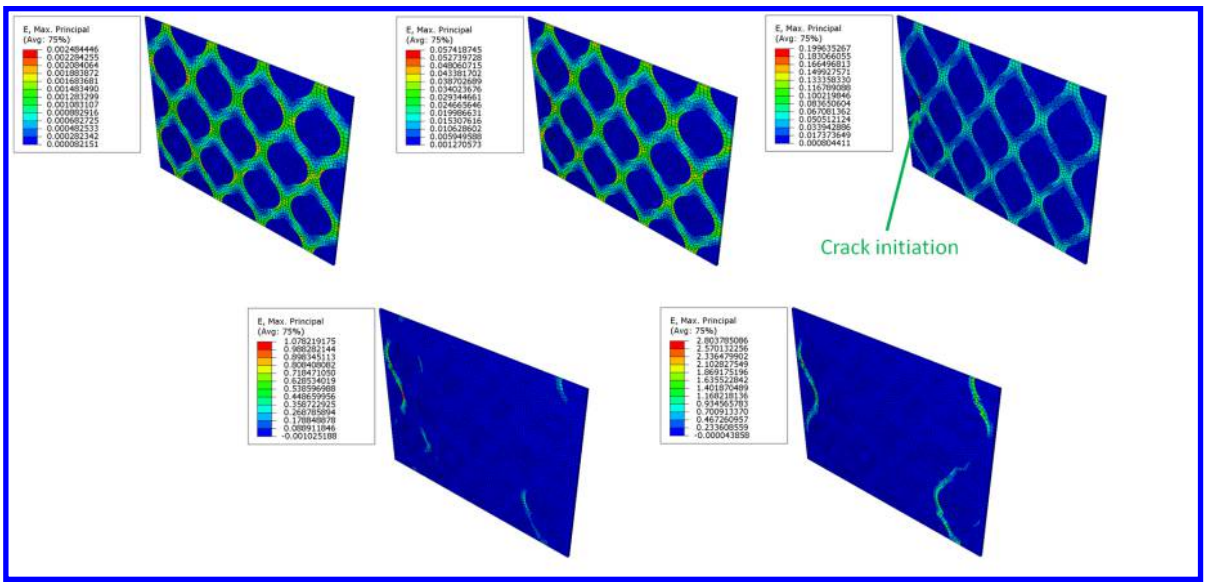

Figure 13. Contour plots of maximum principal strain in Step III along with initial crack initiation site for random RVE - Model 12 (hexagonally packed 16-fiber RVE).

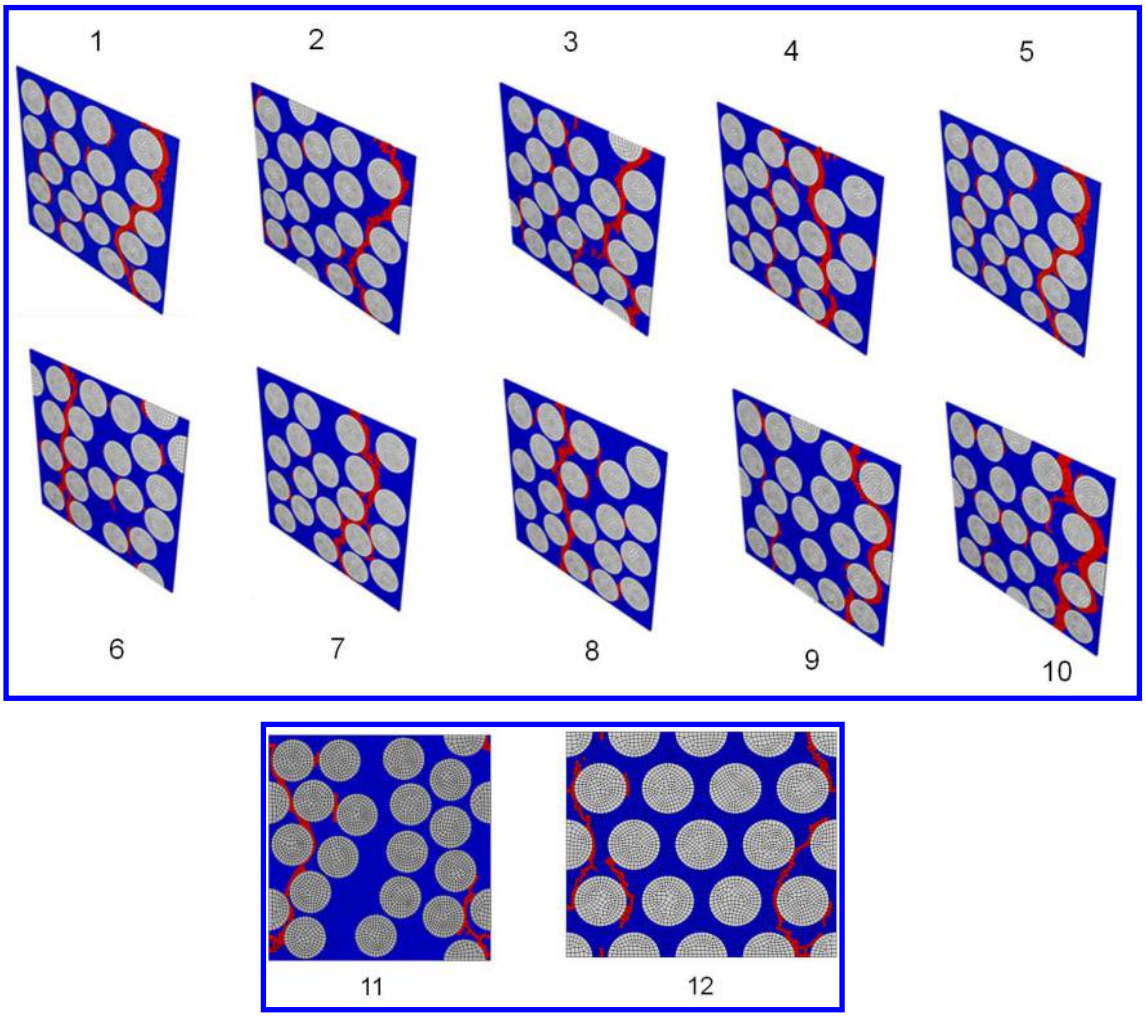

Figure 14. Crack paths in the 12 models when loaded in tension in the transverse direction

values with some metric associated with fiber packing.

References

[1]Song, S., Waas, A. M., Shahwan, K. W., Xiao, X. and Faruque, O., *Braided textile composites under compressive loads: Modeling the response, strength and degradation*, Composite Science & Technology, No. 67, pp. 3059-3070, 2007.

[2]Mei, Y. *Stress evolution in a conductive adhesive during curing and cooling*, Ph.D Thesis, University of Michigan, 2000.

[3]Mei, Y., Yee, A. S., Wineman, A. S. and Xiao, C., *Stress evolution during theromset cure*," Material Research Society symposia proceedings, 1998.

[4]Heinrich, C., Alridge, M., Wineman, A. S., Kieffer, J. Waas A. M. and Shahwan, K. W., *Generation of heat and stress during the cure of polymers used in fiber composites*, International Journal of Engineering Science, Vol. 53, pp. 85 - 111, 2012.

[5]Kamal, M. R., *Thermoset characterization for moldability analysis*, Polymer Engineering & Science, Vol. 14, No. 3, pp. 231-239, 1974.

[6]Hubert, P., Johnston, A., Poursartip, A. and Nelson, K., *Cure kinetics and viscosity models for Hexcel 8552 epoxy resin*, Proceedings of the 46th International SAMPE symposium, Long Beach, CA, pp. 2341-2354, 2001.

[7]Bažant, Z. P., and Oh, B., *Crack band theory for fracture of concrete*, Materials & Structures, Vol. 16, No. 3, pp. 155-177, 1983.